Contents lists available at ScienceDirect

Groundwater for Sustainable Development

journal homepage: http://ees.elsevier.com

Hydrogeochemical and isotopic controls on the source of fluoride in groundwater within the Vea catchment, northeastern Ghana

Musah Saeed Zango [a,*], Kenneth Bayetimani Pelig-Ba [b], Maxwell Anim-Gyampo [a], Abass Gibrilla [c], Emmanuel Daanoba Sunkari [d,e]

[a] Department of Earth Science, Faculty of Earth and Environmental Sciences, CK Tedam University of Technology and Applied Sciences, P.O. Box 24, Navrongo, Ghana
[b] Department of Applied Chemistry and Biochemistry, Faculty of Applied Sciences, CK Tedam University of Technology and Applied Sciences, P.O. Box 24, Navrongo, Ghana
[c] Nuclear Chemistry and Environmental Research Center, National Nuclear Research Institute, GAEC, Box LG 80, Legon-Accra, Ghana
[d] Department of Geological Engineering, Faculty of Engineering, Niğde Ömer Halisdemir University, Main Campus, 51240, Niğde, Turkey
[e] Department of Geological Engineering, Faculty of Mineral Resources Technology, University of Mines and Technology, P.O. Box 237, Tarkwa, Ghana

ARTICLE INFO

Keywords
Groundwater
Fluoride contamination
Stable isotopes
Vea catchment
Ghana

ABSTRACT

Groundwater consumption is considered as a major exposure route to fluoride in humans. Therefore, this study unraveled the sources and sinks of groundwater fluoride in the Vea catchment of northeastern Ghana using an integration of litho-petrography, hydrogeochemical analysis, multivariate statistical analysis, and stable isotope analysis. In this regard, 70 groundwater samples were collected from boreholes and analyzed for major ions and stable isotopes using standard procedures whilst 10 rock samples were collected from the crystalline basement rocks of the Birimian Supergroup and used for the petrographic studies. The petrographic results revealed the dominance of quartz, microcline, plagioclase (albite), biotite, muscovite and hornblende in the lithological units. The order of dominance of fluoride in the various lithologies is K-feldspar-rich granitoid > hornblende-biotite granitoid > basaltic flow > hornblende-biotite tonalite > hornblende biotite granodiorite > biotite granitoid. The groundwater fluoride concentrations varied from 0.35 to 3.95 mg/L with a mean concentration of 1.68 mg/L. Almost 61% of the samples have fluoride concentrations above the World Health Organization's maximum permissible limit of 1.5 mg/L. Groundwater is supersaturated with respect to albite due to silicate weathering and undersaturated with respect to fluorite and calcite. This enhanced ion exchange and fluoride mobilization in the groundwater from progressive calcite precipitation. The fluoride concentrations show positive correlations with Na^+, Mg^{2+}, HCO_3^-, and SO_4^{2-}, confirming that fluoride enrichment is due to silicate weathering and ion exchange reactions. The $\delta^{18}O$ and δ^2H values with respect to V-SMOW vary between −4.15 and −2.75‰ and −22.49 and −13.74‰, respectively suggesting considerable isotopic variation of the groundwater. Enriched isotopic composition is observed with low fluoride concentration whilst depleted isotopic composition is observed with a higher concentration of fluoride in groundwater. The stable isotopic compositions of the groundwater also indicated meteoric origin with an evaporative effect, which partly influences the groundwater chemistry.

1. Introduction

Fluoride (F^-) in drinking water is now a global health concern. Although F^- is required for proper tooth functioning in desired levels, concentrations exceeding 1.5 mg/L may cause significant health problems (WHO, 2017). High levels of F^- occurs in several parts of the world including Africa, Asia, and Middle East (e.g., Adimalla and Li, 2019; Li et al., 2019; Ganyaglo et al., 2019; Zango et al., 2019). In most of these areas, prolonged drinking of groundwater with high F^- levels has led to incidences of dental fluorosis. For instance, in parts of the Indo-Gangetic Alluvial plains, Kumar et al. (2019) reported F^- concentrations up to 5.8 mg/L leading to severe cases of dental fluorosis and bone deformities in children. Based on petrographic analysis of the host rocks in the area as well as molar ratios of chemical species, Kumar et al. (2019) stated that the high groundwater F^- is due to intense water-rock interaction and dissolution from fluoride-bearing minerals in the granitic basement of the Indo-Gangetic Alluvial plains. Similarly, Zango et al. (2019) recently reported high groundwater F^- concentrations up to 13.29 mg/L in the North East Region of Ghana, which causes dental fluorosis in the region, especially among children. They attributed the F^- enrichment to geogenic processes including ion exchange reactions, intense water-rock interactions and mineral disso-

* Corresponding author.
E-mail address: mzango@cktutas.edu.gh (M.S. Zango)

https://doi.org/10.1016/j.gsd.2020.100526
Received 19 August 2020; Received in revised form 16 October 2020; Accepted 6 November 2020
Available online xxx
2352-801/

lution. In the Bongo district of the Upper East Region of Ghana, Sunkari and Abu (2019) also documented high groundwater F^- (up to 4.0 mg/L) in boreholes and indicated that the people are exposed to initial symptoms of dental fluorosis. Like in the North East Region of Ghana, the F^- mobilization in the Bongo district is due to ion exchange reactions and dissolution from fluoride-rich minerals in the Bongo granitoids (Apambire et al., 1997; Craig et al., 2018; Sunkari et al., 2018; Sunkari and Abu, 2019). Elsewhere across the globe, high groundwater F^- has also been linked to dissolution from rocks and ion exchange reactions (e.g., Chae et al., 2007; Farooqi et al., 2007; Thivya et al., 2017; Dehbandi et al., 2018).

Moreover, Saxena and Saxena (2014) mentioned that F^- levels in groundwater are controlled by the climatic conditions of arid to semi-arid areas acting on the regional and local geology coupled with the flow pattern of the groundwater. Groundwater F^- can as well be sourced from igneous and metamorphic rocks with apatite, feldspars, hornblende, pyroxene, biotite, fluorite and clay minerals like illite as the culprits (Thivya et al., 2017). It is also not uncommon to associate groundwater F^- enrichment to the intensity of anthropogenic activities such as industrial and agricultural activities (Kundu and Mandal, 2009).

Assessment of the source of groundwater F^- has been effectively conducted using conventional geochemical graphs, geochemical modeling, multivariate geostatistical analysis, and environmental isotopes (Olaka et al., 2016; Martins et al., 2018; Enalou et al., 2018; Su et al., 2019). Such an integrated approach is able to unravel groundwater flow patterns, recharge sources, effects of evaporation on hydrogeological systems, and thus, the mechanisms responsible for groundwater F^- mobilization.

In the Vea catchment, groundwater is the main potable water supply for domestic purposes considering its relatively cheap cost of abstraction. The people have dug wells for their domestic water supplies and there are several boreholes that are actively in use. However, the exploitation and safety of groundwater in this area is beset with numerous setbacks emanating from interplay of geogenic processes and some anthropogenic activities. There is the possibility of intense dissolution from fluoride-bearing minerals in the Bongo granitoids in the area just as reported in the Bongo district, which is part of the Vea catchment. No readily available research on groundwater quality with respect to contaminants such as fluoride in the entire Vea catchment was found in the literature at the time of this study. Most of the studies are localized, restricted to specific towns and districts in the area or on regional scale. Koffi et al. (2017) conducted a hydrogeochemical study on groundwater and surface water in the Vea catchment but the aim of the study was to assess the quality of the water for domestic and agricultural purposes. Their study did not also determine the fluoride concentrations of the water in the area and thus, the overall quality of the water is not well known. Therefore, the current study seeks to assess the influence of the local geology on the groundwater F^- levels using petrography of the host rocks, hydrochemistry, multivariate statistical analysis and stable isotopes. The study will unravel the mechanisms responsible for F^- mobilization in groundwater of the Vea catchment. Since this is the first study in the area reporting high groundwater F^-, it would serve as a policy framework for stakeholders in the region.

2. Materials and methods

2.1. Study area and climatic conditions

The Vea catchment, which is a sub-catchment of the White Volta Basin in Ghana is a *trans*-boundary catchment covering part of Burkina Faso, Bongo District and Bolgatanga Municipality, both in the Upper East Region, Ghana. In Ghana, the Vea catchment is located between latitudes 10.43°N and 11°N, and longitudes 0.45°W and 1°W (Fig. 1a). The catchment covers a total drainage area of about 305 km^2. The average slope and altitude are 0.2% and 196.5 m a.s.l., respectively. The area is characterized by a single season of rainfall that begins from May and ends in October with an average monthly rainfall of 986 mm. Temperatures are always high and average at 28.6 °C. Nonetheless, monthly averages range from 26.4 °C at the peak of the rainy season in August to an extreme value of 32.1 °C in April (Dickson and Benneh, 1995). As it is common for the tropics, diurnal temperature changes in the area exceed monthly variations (Dickson and Benneh, 1995). The Vea catchment has a total evaporation of 2050 mm, which exceeds the annual rainfall more than two folds.

2.2. Geology and hydrogeology

The Vea catchment is geologically within the Navrongo-Nangodi Greenstone Belt of the Paleoproterozoic Birimian of Ghana (Kesse, 1985). Underlying the catchment are felsic gneisses, basaltic rocks and pyroclastic suite of rocks intruded at places by doleritic dykes, granodiorites (Leube et al., 1990) (Fig. 1a). According to Milési et al. (1989), three types of granitoids intrude in the area, namely; belt-type granitoids, basin-type granitoids, and K-feldspar rich granitoids. The belt and basin type granitoids intrude the volcanic and the metasedimentary suit of rocks, respectively (Fig. 1b). The K-feldspar rich granitoids are very coarse-grained and are identified only in the region and hence, a type locality name of 'Bongo granitoids' is given to them. The belt-type intrusive bodies are composed of hornblende, biotite, plagioclase feldspars and other accessory minerals. On the other hand, the basin-type granitoids are composed largely of potassium feldspar, biotite, and muscovite together with some accessory minerals. These intrusive bodies are coarse to medium-grained. However, the most prominent outcrops in the area are the K-feldspar rich granitoids (Bongo granitoids). Generally, the dominant mineralogical composition of the rocks in the area is potassium and plagioclase feldspars. The rocks in the area have undergone varying degrees of deformations characterized by shearing and jointing. Their coarse nature together with brittle deformations also makes them porous. These deformational features and the porous fabric serve as conduits/channel ways for water to readily infiltrate the rocks thereby facilitating chemical alteration of the mineral constituents.

The Vea catchment forms a significant part of the crystalline basement aquifers in northern Ghana where the aquifers are mainly within the weathered rocks that are overprinted by unique fractures. Storage of groundwater in the rocks is generally very poor but increases at the zone of the weathered and fractured rocks. Groundwater occurrence in the area depends largely on the thickness of the overburden and the degree of fracture of bedrocks. Recharge is from direct precipitation and the main Vea dam that frequently gets flooded during the rainy season. Sunkari and Abu (2019) stated that the average recharge is approximately 4% of the total annual precipitation that is 40 mm/year. Higher water levels are restricted to areas with higher granitic elevation maybe due to increasing rates of recharge alongside decreasing horizontal conductivity (Martin and Van De Giesen, 2005). Borehole yields are low ranging from 0.13 to 0.32 L/s but then are sufficient for installation of hand pumps (Apambire et al., 1997).

2.3. Petrographic studies

Geological field mapping exercise was carried out in March 2019 during the dry season when the grasses within the study area were dry and burnt in isolated areas, this made movement in the field easy and outcrops visible and accessible. During the sample collection, efforts were made to take fresh/relatively fresh rock samples, 10 samples were collected and thin sections prepared. The thin sections were petrographically studied using reflected light microscope at the department of Earth Science, University of Ghana.

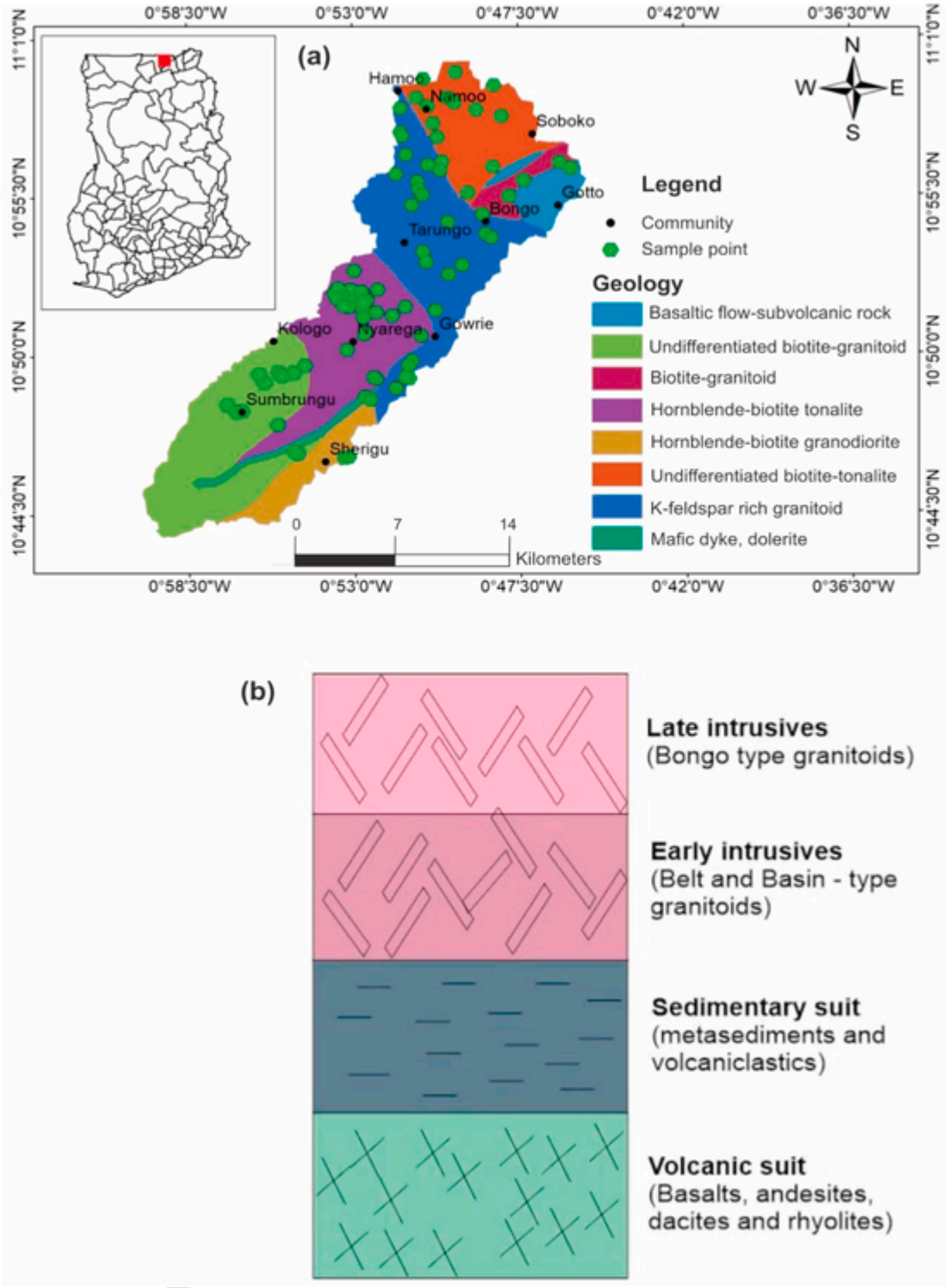

Fig. 1. (a) Location and geological map of the Vea catchment showing the sample points (b) schematic general lithostratigraphic section of the study area.

2.4. Geochemical analysis of groundwater samples

Groundwater sampling was carried out at the peak of the dry season in March 2019. A total of seventy (70) water samples were collected from boreholes in the area. Major dissolved elements were analyzed for all the 70 samples. Alkalinity and physical parameters such as electrical conductivity (EC), total dissolved solids (TDS), temperature and pH of the samples were measured in situ using HACH field titration kit and portable EC and pH meters. Groundwater samples from boreholes were subsequently filtered through 0.45 μm membranes and collected in pre-conditioned polyethylene bottles. Filtered and acidified (1% v/v HNO_3) samples were used for major cations, while filtered unacidified samples were used or anion analysis. Na^+ and K^+ were analyzed using flame photometer, Ca^{2+}, and Mg^{2+} were determined by EDTA titration. Major anions (Cl^-, SO_4^{2-}, HCO_3^-, F^-, and NO_3^-) were determined using

Dionex ICS 90 ion chromatography system at the Ghana Atomic Energy Commission in Accra. The data was supplemented from the database of community water and sanitation agency (CWSA) in the Upper East Region of Ghana. In order to maintain the accuracy and a degree of confidence in the integrity of the data, all the sampling bottles and glassware were soaked in a 5% nitric acid for a day and rinsed with deionized water before use. Instruments used were calibrated with standard chemical solutions prepared from commercially available chemicals and validated with Standard Reference Materials (SRM) and Certified Reference Materials (CRM). The SRM were analyzed repeatedly at predetermined intervals to confirm that the method remained in a state of statistical control. Duplicate samples were also measured and compared and their results were found reproducible within ±5% error limit. Again, accuracy of the laboratory analysis was checked using the anion-cation balance method and only those results within ±5% were relied on for subsequent interpretation.

2.5. Stable isotope analysis

During the sample collection in the field, separate samples were collected in tightly capped 20 ml HDPE bottles. The isotope analysis involved oxygen and hydrogen isotopes of sixty-nine (69) samples. The water samples collected were analyzed using a Los Gatos Research DLT-100 liquid isotope water analyzer at the Ghana Atomic Energy Commission in Accra. The analyzer was coupled to a CTC LC-PAL liquid auto-sampler (Los Gatos Inc., CA). Pre-calibrated internal laboratory standards and a blank were used in sample runs and the results were normalized to the VSMOW-SLAP δ scale. The analytical precision was ±0.1‰ and ±0.3‰ for the oxygen and hydrogen isotopes, respectively. The detailed method of measurement is described in IAEA (2009).

2.6. Data analysis

The hydrochemical data was interpreted by means of ternary Piper diagram (Piper, 1953) and bivariate plots using AquaChem software version 4.0. Groundwater F^- spatial distribution map was generated using kriging interpolation technique with Surfer software version 13. Kriging was the choice of interpolation technique since it uses semi-variograms in solving surface estimation problems (Sunkari and Abu, 2019; Sunkari et al., 2020). The saturation indices of the mineral phases identified in the water samples were calculated using PHREEQC software (Parkhurst and Appelo, 1999). Multivariate statistical analysis involving Pearson correlation and R-mode factor analysis were used in understanding the inter-ion relationships and associations as well as deducing the sources of the ions. During the R-mode factor analysis, principal component analysis was the extraction method used whereas Varimax rotation was the rotation technique. In order to minimize the number of factors to extract in the R-mode factor analysis, Kaiser Criterion (Kaiser, 1960) was employed because the Kaiser Criterion filters out factors with initial eigenvalues <1.0. The multivariate statistical analysis was performed using SPSS Statistics version 25. The origin of the groundwater was understood by the stable isotope patterns of the samples. AquaChem software version 4.0 was used in producing cross plots of the isotopes and other ions. Global Meteoric Water Line (GMWL) was taken from Craig (1961) from the equation below.

$$\delta^2H = 8\delta^{18}O + 10 \quad (1)$$

where δ is the enrichment parameter of the isotope, H and O are the heavy isotopes of hydrogen and oxygen, respectively.

However, since the GMWL is a line of best fit used globally, it may not reflect the local conditions in the study area, hence the Local Meteoric Water Line (LMWL) proposed by Akiti (1986) for Ghana defined by equation (2) was used in this study.

$$\delta^2H = 7.86\delta^{18}O + 13.61 \quad (2)$$

3. Results and discussion

3.1. Petrography

The petrographic results (Fig. 2) indicate the presence of quartz > microcline > plagioclase > biotite > muscovite > hornblende > opaque minerals and other accessory minerals. Quartz is the source of SiO_2 although there is no major element geochemical data to support this claim. The feldspars (microcline and plagioclase-Na bearing feldspar, albite) are the source of K^+ and Na^+, respectively. This is due to the nature of the twinning, that is, tartan and polysynthetic twining of the microcline and albite (plagioclase) of these minerals under reflected light. These minerals contribute to F^- levels in groundwater according to Ozsvath (2006) and Chae et al. (2006). Based on the textures and mineral assemblages of the studied samples, the samples are sub-euhedral coarse-textured and largely leucocratic. The leucocratic nature is due to the large quartz and microcline content. There are largely anhedral textures of biotite, muscovite and hornblende in majority of the samples. These anhedral textures are due to the readily alteration of the minerals due to the unstable nature of the minerals in the granitic rocks upon exposure to agents of chemical alteration like water. The diversified mineralogical composition of these samples suggests the formation of the minerals at different times and temperature and this informs their level of stability with respect to chemical alteration. There is the presence of accessory chlorite, sericite, and epidote, which are alteration minerals of biotite, feldspars (microcline and plagioclase/albite) and hornblende (Fig. 2). The dominance of the minerals (Table 1) is as follows; quartz (41%), microcline (31%), plagioclase (17.2%), biotite (3.1%), muscovite (2.2%) and hornblende (1.2%) in the lithological units. The order of dominance of fluoride in the various lithologies is K-feldspar-rich granitoid (Bongo Granite) > hornblende-biotite granitoid > basaltic flow > hornblende-biotite tonalite > hornblende biotite granodiorite > biotite granitoid (Table 2).

3.2. Hydrochemistry

The statistical summaries of the hydrochemical parameters are presented in Table 3 whereas the concentrations of all the hydrochemical parameters are given in supplementary Table 1. The pH of the water varies from 7.03 to 7.74 with a mean value of 7.30 consistent with the WHO acceptable range of 6.5–8.5 (WHO 2017). Such range of pH suggests that the water is near-neutral to slightly alkaline. The moderate alkaline pH may be due to dissolved clays and carbonates associated with the metasedimentary rocks, which serve as appropriate medium for adsorption and desorption of metals and toxic ions like fluoride in groundwater (Keshavarzi et al., 2010; Zango et al., 2019). The temperature of the water varies from 24.2 to 31.3 °C with a mean of 27.2 °C. The EC values range from 176 to 1352 μS/cm with a mean value of 400 μS/cm falling within the guideline value of 2500 μS/cm (WHO 2017). The TDS concentrations (96.8–744 mg/L, mean of 221 mg/L) were also generally low and the groundwater can be described as fresh based of Freeze and Cherry (1979) classification. The low TDS values are also likely due to the short residence time of the groundwater limiting intense water-rock interaction (Sunkari et al., 2019). The well depths range from 17.0 to 70.0 m with a mean of 42.8 m and from the supplementary Table 1, it is observed that the deeper the well, the higher the major ion concentrations. In terms of

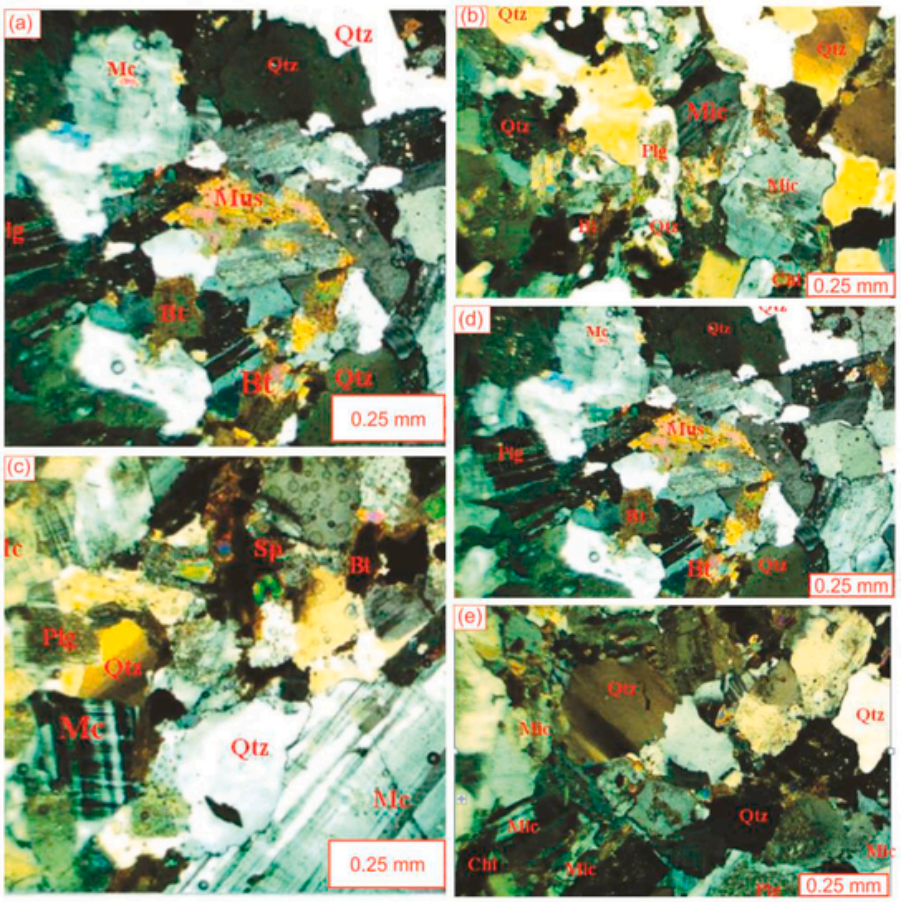

Fig. 2. Photomicrographs of the studied samples of the Vea catchment (Qtz = quartz, Mic = microcline, Plg = plagioclase, Bt = biotite, Mus = muscovite, Chl = chlorite, Sp = sphene).

Table 1
Model composition of minerals in the Vea catchment.

Sample ID		PAZ001	PAZ002	PAZ003	PAZ004	PAZ005	PAZ006	PAZ007	PAZ008	PAZ009	PAZ010	Average
Modal composition (%)	Microcline	36	32	30	42	36	52	34	28	20		31
	Quartz	40	50	44	36	42	28	24	36	55	55	41
	Plagioclase	19	14	18	15	14	17	20		20	35	17.2
	Hornblende	0			4	3					5	1.2
	Biotite	4	4	5	2	4	2			5	5	3.1
	Sphene			1	<1	<1			4			0.5
	Chlorite	<1							19			1.9
	calcite							<1				
	Epidote						<1		12			1.2
	Muscovite			2				20				2.2
	Opaque mineral	<1					<1	<1	<1			

major cation concentrations, Na^+ is the dominant cation with concentrations ranging from 10.9 to 211 mg/L and a mean concentration of 38.6 mg/L (Table 3). The WHO guideline value for Na^+ in drinking water is 200 mg/L (WHO 2017), implying that some of the samples exceeded the guideline value. Such a trend is probably from silicate weathering from the granitoids in the area. Ca^{2+} is the second most abundant cation in the groundwater varying from 1.40 to 26.8 mg/L with a mean value of 9.95 mg/L, falling within the WHO maximum permissible limit of 200 mg/L (Table 3). The Mg^{2+} concentrations also vary from 1.02 to 28.5 mg/L with a mean concentration of 7.14 mg/L (Table 3). K^+ is the least dominant cation in the groundwater with concentrations in the range of 0.49–5.20 mg/L and a mean value of 1.97 mg/L far below the standard guideline value of 200 mg/L (Table 3). In all, the major cation concentrations vary in the order of $Na^+ > Ca^{2+} > Mg^{2+} > K^+$, suggesting rapid release of Na from albite via alteration and leaching processes (Fig. 2). Although K-bearing microcline is dominant, it is not contained in the high temperature minerals like Ca-bearing anorthite, Na-bearing albite and Mg-bearing biotite/hornblende. Hence, it is relatively stable compared to these minerals and as such will be released last and possibly less into groundwater.

Table 2
Summary statistics of stable isotopes and fluoride concentrations in groundwater within the Vea catchment.

	Hornblende-biotite granitoid (n = 14)	K-feldspar -rich granitoid (n = 21)	Basaltic flow (n = 4)	Hornblende-biotite tonalite (n = 17)	Biotite granitoid (n = 11)	Hornblende-biotite granodiorite (n = 3)
Fluoride						
Minimum	0.55	0.52	0.59	0.35	0.43	0.58
Maximum	3.78	3.95	3.15	2.54	0.85	1.90
Average	2.26	1.71	2.07	1.64	0.64	1.46
$\delta^{18}O$						
Minimum	−3.36	−4.04	−3.28	−4.15	−3.93	−3.72
Maximum	−3.11	−2.76	−3.16	−3.11	−2.75	−3.49
Average	−3.55	−3.46	−3.23	−3.63	−3.33	−3.64
$\delta^{2}H$						
Minimum	−17.4	−22.5	−17.4	−22.3	−21.5	−22.0
Maximum	−15.9	−14.3	−16.1	−15.0	−13.7	−16.3
Average	−19.8	−17.9	−16.7	−18.6	−17.5	−18.9

Table 3
Summary statistics of the hydrochemical parameters and saturation indices of the mineral phases (STD = Standard deviation, WHO = World Health Organization).

Parameter	Unit	No	Min	Max	Mean	STD	WHO (2017)
pH	–	70	7.03	7.74	7.30	0.17	6.5–8.5
Temp.	˚C	70	24.2	31.3	27.2	2.97	NA
EC	μS/cm	70	176	1352	400	180	2500
TDS	mg/L	70	96.8	744	220	98.7	500
Na^+	mg/L	70	10.9	211	38.6	28.9	200
K^+	mg/L	70	0.49	5.20	1.97	0.89	200
Ca^{2+}	mg/L	70	1.40	26.8	9.95	6.40	200
Mg^{2+}	mg/L	70	1.02	28.5	7.14	5.68	NA
Cl^-	mg/L	70	14.7	178	37.0	24.4	250
HCO_3^-	mg/L	70	30.0	260	80.0	43.0	NA
SO_4^{2-}	mg/L	70	1.01	62.9	9.29	9.22	200
F^-	mg/L	70	0.35	3.95	1.66	0.92	1.5
NO_3^-	mg/L	70	3.29	54.7	16.3	11.4	50
Well depth	m	53	17.0	70.0	42.8	15.8	
SI Albite		70	−0.32	5.59	1.38	1.01	
SI Calcite		70	−2.72	0.06	−1.21	0.55	
SI Dolomite		70	−3.97	−0.13	−2.38	0.99	
SI Fluorite		70	−2.26	−0.19	−1.33	0.54	
SI Gypsum		70	−6.24	−1.67	−3.4	0.7	
SI Halite		70	−9.08	−5.43	−7.65	0.59	

HCO_3^- is the most abundant major anion in the groundwater with concentrations in the range of 30.0–260 mg/L and a mean concentration of 80.0 mg/L (Table 3). This might be due to limited dissolution of carbonate minerals in the aquifer system since the area contains no carbonate rocks (Fig. 1). The Cl^- concentrations range from 14.7 to 178 mg/L with a mean concentration of 37.0 mg/L, falling within the WHO guideline value of 250 mg/L (Table 3). Similarly, the SO_4^{2-} concentrations (1.01–62.9 mg/L with a mean value of 9.29 mg/L) are also within the WHO maximum permissible limit of 200 mg/L (Table 3). Perhaps ion exchange reactions or limited dissolution of gypsum are the culprits for the SO_4^{2-} concentrations in the groundwater. Other anions of importance in groundwater studies are F^- and NO_3^- since their concentrations can affect the health of consumers of the water. Therefore, the F^- concentrations of groundwater in the Vea catchment vary from 0.35 to 3.95 mg/L with a mean concentration of 1.66 mg/L (Table 3). This suggests that the water is contaminated with F^- since the maximum permissible limit of F^- in drinking water is pegged at 1.5 mg/L (WHO, 2017). Worryingly, the mean concentration (1.68 mg/L) exceeds the guideline value (1.5 mg/L) exposing the people to the threat of dental fluorosis. The high fluoride samples are mostly within the area dominated by K-feldspar-rich granitoid (Bongo Granite) and hornblende-biotite granitoid (Fig. 1; Table 2). The NO_3^- concentrations (3.29–54.7 mg/L, mean value of 16.3 mg/L) also exceed the acceptable limit of 50 mg/L (Table 3). The relatively high NO_3^- concentrations may be due to leaching from nitrate fertilizers (Sunkari et al., 2020) applied on farms in the Vea catchment. Altogether, the major ion concentrations in groundwater of the Vea catchment vary in the order of $HCO_3^- > Cl^- > SO_4^{2-}$.

3.3. Geochemical evolution of groundwater

Ternary Piper diagram (Piper, 1953) has been widely used in groundwater studies to discriminate the various hydrochemical facies and geochemical evolution of groundwater in aquifer systems. Therefore, this study also used Piper diagram to show the type of water in the Vea catchment. From the Piper diagram (Fig. 3), the dominant hydrochemical facies is Na–Ca–HCO_3 (85%) followed by Ca–Na–Mg–HCO_3 (10%) and Mg–Na–HCO_3 (5%). The dominance of Na–Ca–HCO_3 water type might be due to silicate weathering and ion exchange reactions in the aquifer. Similar reason may be accounting for the other two types of water in the area. Koffi et al. (2017) studied the hydrochemistry of some parts of the Vea catchment and mentioned that the dominant hydrochemical facies in the Vea catchment is Ca–Mg–HCO3 water. They also linked the dominance of the Ca–Mg–HCO3 water type to cation exchange and silicate weathering, which is consistent with the findings of this study.

3.4. Groundwater fluoride distribution

A total of 43 samples out of the 70 samples under this study have groundwater F^- above 1.5 mg/L. This implies that about 61% of the people in the communities where the groundwater was sampled from the entire Vea catchment is drinking water that is detrimental to their health. The affected communities are mostly around the northeastern, central, and southwestern parts of the study area (Fig. 4). The major communities in these areas include Bongo, Vea Nzangongo, Balungu, Kodorogo, Tarungo, Nyarega, and Sumbrungu (Fig. 4). Areas with groundwater F^- between 1.5 and 2.4 mg/L include Namoo Amokobisi 1, Namoo Yakabisi, Sambolingu Kansoe, Sambolingu Amanga, Bungu, Balungu Doni, Balungu, Langanabisi, Bongo Nabisi, Zoko Tarongo, Bogorodo, Namoo Amokobisi 2, Boko Tendama 2, Gowri, Vea Akugrebisi, Vea Gunga, Vea Asornabisi, Bongo SHS 2, Nabiisi Pri/JHS, Sumbrugu

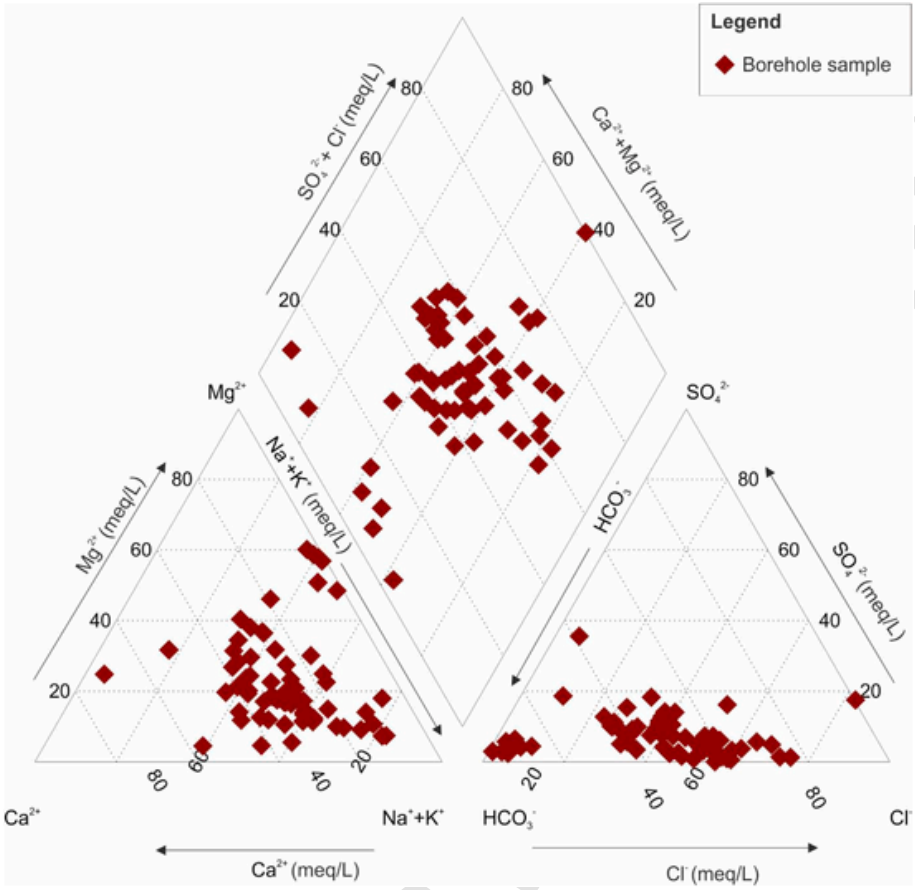

Fig. 3. Ternary Piper diagram (Piper, 1953) showing the various types of water in the Vea catchment.

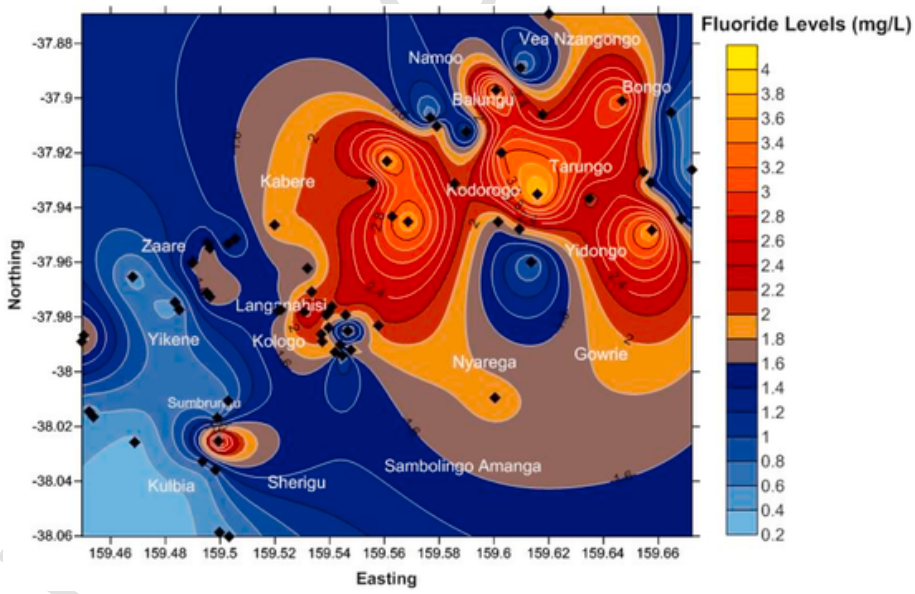

Fig. 4. Spatial distribution of groundwater fluoride in the Vea catchment of northeastern Ghana.

Pri/JHS, Konvi Longo, Zoono Control, Sherigu Dorungu 1, Sherigu Dorungu 2, Zaare Ayombisi 1, Zaare Ayombisi 2, Zaare Ayorogobisi 1, Zaare Ayorogobisi 2, Zaare Amoabisi 1, Zaare Amoabisi 2, Zaare Nyarega 1, Nyarega 1, and Nyarega 2 (Fig. 4). However, areas with groundwater F^- between 2.5 and 3.9 mg/L include Balungu CHPS, Bongo SHS 1, Kabere CHPS, Kodorogo CHPS, St. Annes Pri/JHS, Vea Kupielga, Nyarega Asammabisi, Akanweebisi, Dulungu Naabis, and Sumbrungu Amogribisi (Fig. 4). All these communities are intruded by K-feldspar-rich granitoid (Bongo Granite) and hornblende-biotite granitoid (Fig. 1) indicating possible intense dissolution. It is indeed worrying that boreholes in public schools and health care centers in the area are all extremely contaminated with F^-. Though this study did not conduct a medical assessment of the teeth of the people in the area, it was observed that most of the children and even adults have mottled teeth,

which is likely evidence for dental fluorosis. The Vea catchment is not precluded from the menace of dental fluorosis as observed in most parts of the Upper East Region. Majority of the people have mottled teeth but are unaware of the cause of such ailment. The rural people believe that it is a curse from their gods and ancestors and the elite in the society rather attribute it to poor dental care at homes. However, the severity of the issue suggests that none of the reasons given by the inhabitants may be accounting for the incidence of dental fluorosis.

3.5. Controlling factors of groundwater chemistry

Gibbs plots (Gibbs, 1970) have been effectively used over the years to decipher the implication of weathering, evaporation and dilution on groundwater chemistry. On the Gibbs plots (Fig. 5a and b), the studied samples of the Vea catchment largely support water – rock interaction as the dominant process controlling the elevated F^- contents in the groundwater with one sample indicating evaporation dominance. The effect of water – rock interaction on F^- levels in groundwater has been extensively studied in the literature (Shah and Danishwar, 2003; Sunkari et al., 2018; Sunkari and Abu, 2019; Zango et al., 2019). A plot of the F^- concentrations (mg/L) against the well depths (m) reveals a linear relationship ($r = 0.41$) where an increase in the F^- concentrations (>1.5 mg/L) is associated with increasing well depth although some shallow wells also have high F^- concentrations (Fig. 5c). This might be pointing to the longer groundwater residence times and thus, intense water-rock interaction and ion exchange reactions in the aquifer. However, the shallow wells with high F^- concentrations (>1.5 mg/L) may be as a result of anthropogenic activities around the aquifer.

When equilibrium is reached between Na^+ and F^-, the high Na^+ released into groundwater could produce soft water thereby facilitating higher F^- concentration levels (Naseem et al., 2010). Na/(Na + Cl) ratio is a suitable proxy in discriminating origins of groundwater (Hounslow, 1995). The average Na/(Na + Cl) ratio of the groundwater is 0.53 supporting the influence of albite on the groundwater chemistry. F^- concentrations are found to be higher in granitic rocks than any other rock type with a range of 500 and 1400 mg/kg (Koritnig, 1978; Krauskopf and Bird, 1995). High levels of F^- in aquifers have been attributed to biotite dissolution and fluoride replacement of OH^- sites due largely to their similar ionic radii, F^- = 1.23–1.36 Å and OH^- = 1.37–1.40 Å (Li et al., 2003; Naseem et al., 2010; Kumar et al., 2018). This fluoride enrichment process is time dependent as prolonged residence time of biotite-bearing rocks is reported to have resulted in elevated F^- levels (Raju et al., 2009; Rao et al., 2017; Kumar et al., 2018) following the chemical reaction below:

$$KMg_3[AlSi_3O10]F_2 + 2OH^- \rightarrow KMg[Al_2Si_3O_{10}][OH]3 + 2F^- \quad (3)$$

About 61% of borehole samples have elevated levels of F^- above the acceptable levels of 1.5 mg/L (Table 3), and this is due to biotite dissolution and evaporation from the aquifers (Young et al., 2011). This is consistent with the dominance of hornblende-biotite granitoid in the area (Fig. 1) and the high amount of fluoride (up to 3.78 mg/L) released from these rocks into groundwater (Table 2).

The presence and contribution of mafic and ultramafic minerals to the F^- levels in the area is shown by the low Mg/(Ca + Mg) ratio of 0.37 suggesting trace content of biotite and hornblende minerals in the area (Fig. 2). Alteration of microcline, albite and muscovite into clay minerals such as smectite and kaolinite, particularly kaolinite can release F^- bearing minerals from granitic rocks via the process of kaolinization and concentrate it in groundwater. The area has huge deposits of kaolinite in the Balungu and Vea dam flood plain with a river serving as a source of water to the Vea dam. The elevated levels of F^- within the catchment could be attributed partly to the process of kaolinization. The effect of silicate weathering on groundwater F^- con-

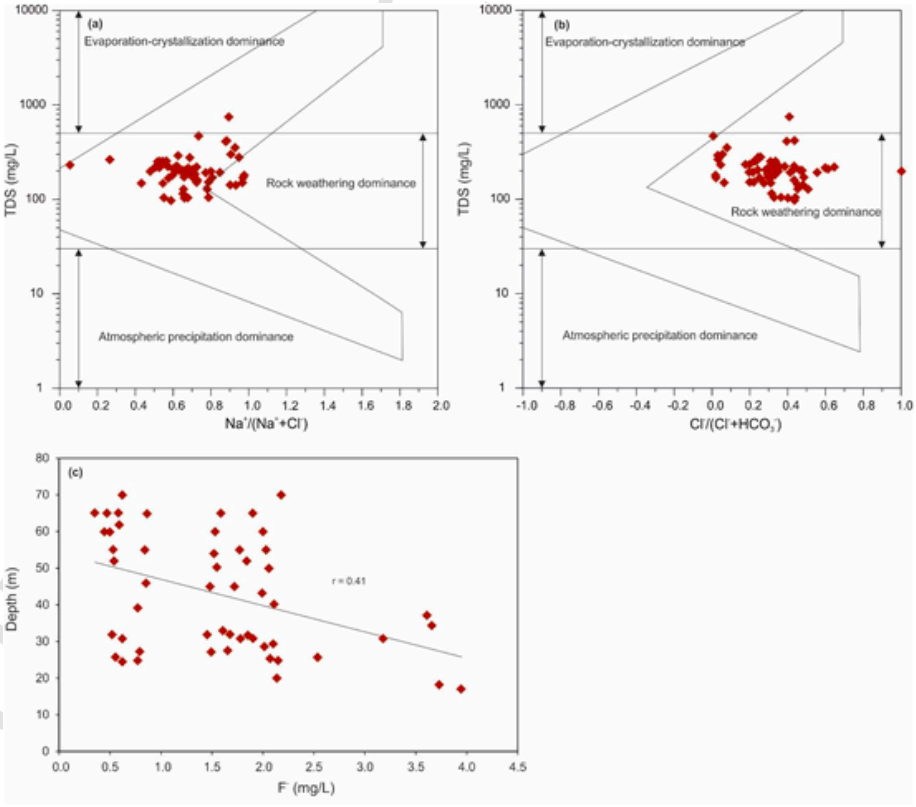

Fig. 5. Gibbs plots (Gibbs, 1970) indicating the dominant mechanisms influencing the groundwater chemistry (a) cations and (b) anions, and (c) Well depths (m) versus F^- concentrations (mg/L) confirming longer groundwater residence time and intense water-rock interaction.

centration has been constrained using Na^+/Cl^- ratio. When the ratio Na^+/Cl^- values > 1, this is indicative of silicate weathering and halite dissolution (Naseem et al., 2010; Kumar et al., 2018). Almost all the studied samples have Na^+/Cl^- values > 1 (Fig. 6a); this is due to the weathering of the felsic gneisses in the area, which subsequently leached the excess Na^+ into the groundwater. The high Na^+/Cl^- molar ratio also indicates that apart from silicate weathering, halite dissolution was also responsible for the elevated Na^+ and Cl^- concentrations in the groundwater. The dominance of silicate weathering in the area as revealed in this study is consistent with the findings of Koffi et al. (2017). Additionally, all the samples plot above the 1:1 line except two samples on the Na^+ (mg/L) and Cl^- (mg/L) bivariate plot (Fig. 6a), implying the dominance of ion exchange reactions enriching these ions. The two samples that plot below the 1:1 line are due to reverse ion exchange reactions that provided the excess Na^+ and Cl^-. The plotting of some of the samples in close proximity to the 1:1 line further highlights the effect of halite dissolution on the groundwater chemistry. The molar ratios of Na^+/Ca^{2+} are also greater than 1 for all the samples indicating low calcium activity (Fig. 6b). The high Na^+/Ca^{2+} molar ratios also point out the prevalence of ion exchange reactions in the aquifer considering the plotting of majority of the samples above the 1:1 line on the Na^+ (mg/L) and Ca^{2+} (mg/L) bivariate plot (Fig. 6b). However, just as observed in the Na^+ (mg/L) and Cl^- (mg/L) bivariate plot, the three samples that plot below the 1:1 line on the Na^+ (mg/L) and Ca^{2+} (mg/L) bivariate plot reveal that reverse ion exchange is responsible for the Na^+ and Ca^{2+} concentrations of those samples.

A plot of Na^+ (mg/L) versus HCO_3^- (mg/L) (Fig. 6c) indicates that the excess HCO_3^- resulted from calcite precipitation, which eventually reduced the Ca^{2+} concentration relative to the Na^+ concentration (Younas et al., 2019). This is a clear evidence for the reverse ion exchange process observed in the Na^+ (mg/L) versus HCO_3^- (mg/L) bivariate plot (Fig. 6c). The dominant role of silicate weathering, especially weathering of the granite gneisses on the groundwater chemistry is further constrained on the bivariate plot of the molar ratios of Mg^{2+}/Na^+ and Ca^{2+}/Na^+ (Fig. 6d). On this diagram carbonate dissolution appears to influence the chemistry of only two samples. Moreover, bivariate plot of $(Ca^{2+} + Mg^{2+})$ and $(SO_4^{2-} + HCO_3^-)$ gives a hint that the samples with F^- concentrations above 1 fall below the 1:1 equiline (Fig. 6e). This confirms the silicate weathering and base ion exchange reactions dominant in the aquifer that progressively elevated the HCO_3^- and F^- concentrations in groundwater. The effect of dolomitization on the groundwater chemistry cannot be precluded in the Vea catchment since majority of the samples plot along the 1:1 line (Fig. 6e). However, de-dolomitization facilitated the removal of excess Ca^{2+} and Mg^{2+} in the water and enhanced the addition of Na^+ via ion exchange in the recharging freshwater (Zango et al., 2019). The Ca^{2+} and SO_4^{2-} concentrations may also be as a result of dissolution of gypsum since majority of the samples plot close to and along the 1:1 line on the Ca^{2+} and SO_4^{2-} cross plot (Fig. 6f). Nevertheless, it is worthy to mention that reverse ion exchange and perhaps anthropogenic input from decomposed sulfates in fertilizers may also account for the groundwater SO_4^{2-} enrichment (Laxmankumar et al., 2019).

3.6. Sources of groundwater fluoride

About 61% of the boreholes in the Vea catchment that intersect biotite-rich granitoids contain F^- levels above the maximum permissible limit of 1.5 mg/L. This jeopardizes the health and livelihood of the rural folks that dwell on the water for domestic purposes. The high groundwater F^- occurred under alkaline conditions (pH = 7.03–7.74). It is widely reported that alkaline conditions (increase in pH) favor groundwater F^- mobilization (Keshavarzi et al., 2010; Kumar et al., 2018; Zango et al., 2019). As stated earlier, the Vea catchment contains high amounts of clay minerals and thus, the alkaline pH alongside the presence of the clays may be a control mechanism for the F^- mobilization in the groundwater. Keshavarzi et al. (2010) stated that F^- has the proclivity of getting adsorbed on clay mineral surfaces in alkaline water. This implies that the high F^- concentrations in the studied groundwater might be as a result of F^- adsorption on the surfaces of clay minerals under the dominant alkaline conditions in the area. This is supported by the positive correlation (r = 0.19) between pH and F^- (Table 4). Also, the increase in pH, Na^+, and HCO_3^- eventually in-

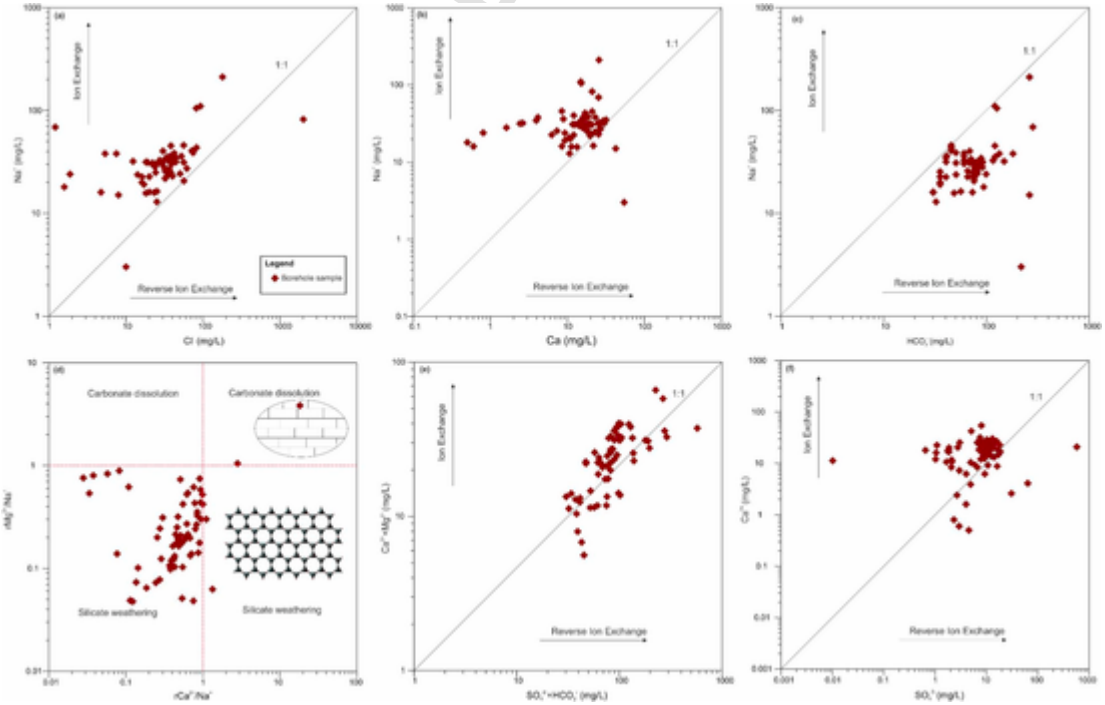

Fig. 6. Relationships among the major ions in the groundwater.

Table 4
Pearson correlation matrices of the hydrochemical parameters (numbers in bold indicate correlation coefficients ≥ 0.70).

	pH	Temp.	EC	TDS	Na^+	K^+	Ca^{2+}	Mg^{2+}	Cl^-	HCO_3^-	SO_4^{2-}	F^-	NO_3^-
pH	1												
Temp.	0.24	1.00											
EC	0.36	0.20	1.00										
TDS	0.36	0.20	**1.00**	1.00									
Na^+	0.19	0.07	**0.91**	**0.91**	1.00								
K^+	0.17	0.14	0.18	0.18	0.13	1.00							
Ca^{2+}	0.14	−0.09	0.03	0.03	−0.08	0.07	1.00						
Mg^{2+}	0.31	0.22	0.42	0.42	0.10	0.13	−0.19	1.00					
Cl^-	0.12	−0.04	**0.79**	**0.79**	**0.87**	0.26	0.04	0.10	1.00				
HCO_3^-	0.48	0.25	**0.92**	**0.92**	**0.78**	0.11	−0.04	0.47	0.55	1.00			
SO_4^{2-}	0.07	0.18	0.30	0.30	0.16	−0.11	−0.04	0.42	−0.03	0.32	1.00		
F^-	0.19	0.04	0.22	0.22	0.19	0.00	−0.69	0.29	0.01	0.40	0.24	1.00	
NO_3^-	0.05	0.06	0.19	0.19	0.09	0.17	0.50	0.22	0.08	0.05	0.06	−0.53	1.00

creases groundwater F^- concentrations via the aforementioned mechanisms in the previous section.

From the Gibbs plots, it is observed that water-rock interaction is the dominant geochemical process residing in the hydrogeological system of the Vea catchment. Such process is common in semi-arid environments where ion exchange reactions involving Ca^{2+} and Na^+ result in the reduction of Ca^{2+} and the enrichment of Na^+ and F^- (Karro and Uppin, 2013). The possible cation exchange reaction that took place between Ca^{2+} and Na^+ is supported by the dominance of Na-bearing plagioclase (Fig. 2) and the high content of Na^+ with a mean of 40.3 mg/L relative to the mean Ca^{2+} concentration of 24.5 mg/L (Table 3). Additionally, the F^- concentrations show positive correlations with most of the hydrochemical parameters including EC, TDS, Na^+, Mg^{2+}, HCO_3^-, and SO_4^{2-} (Table 4) indicating that F^- enrichment is related with the mechanisms enriching these parameters in the water. As explained above, most of these hydrochemical parameters are enriched in the water via ion exchange reactions and similar explanation can be given to the groundwater F^- enrichment. Nevertheless, negative correlation of F^- with K^+ and Ca^{2+} (Table 4) implies reverse ion exchange reactions in the aquifer system.

Geochemical modeling is widely used in groundwater studies to calculate the saturation indices (SI) of mineral phases residing in water and contributing to groundwater F^- enrichment (Younas et al., 2019; Zango et al., 2019). The mineral phases identified in the water include albite (SI = −0.32 to 5.59, mean = 1.38), calcite (SI = −2.72 to 0.06, mean = −1.20), dolomite (SI = −3.97 to −0.13, mean = −2.38), fluorite (SI = −2.26 to −0.19, mean = −1.33), gypsum (SI = −6.24 to −1.67, mean = −3.40), and halite (SI = −9.08 to −5.43, mean = −7.65) (Table 3), suggesting that all the samples are undersaturated with respect to these minerals except albite and calcite. On a bivariate plot of the SI calcite versus F^- (mg/L), all the samples plot in the calcite undersaturation zone except one sample that plots in the calcite saturation zone (Fig. 7a). Similarly, all the samples appear to fall within the fluorite undersaturation zone in the SI fluorite versus F^-

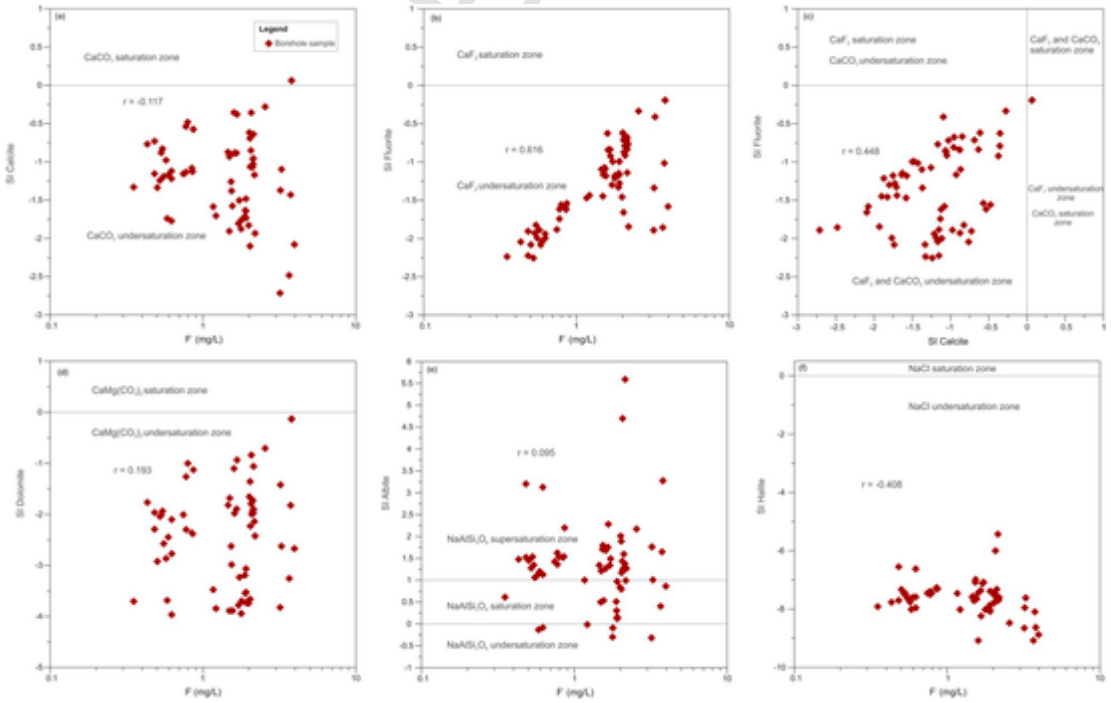

Fig. 7. (a) Bivariate plot of saturation index (SI) of calcite ($CaCO_3$) and F^- (mg/L), (b) SI fluorite (CaF_2) and F^- (mg/L), (c) SI CaF_2 against SI $CaCO_3$, (d) SI dolomite [CaMg(CO3)2] and F^- (mg/L), (d) SI albite ($NaAlSi_3O_8$) and F^- (mg/L), (e) SI halite (NaCl) and F^- (mg/L).

(mg/L) plot (Fig. 7b). The results clearly elucidate that groundwater in the Vea catchment evolved under alkaline conditions where most of the samples are undersaturated with respect to calcite, which enhanced progressive removal of Ca^{2+} and preferential release of F^- in solution. In such a scenario, the groundwater retains higher F^- concentrations prior to saturation with fluorite. It is suggested that fluorite dissolution in the Vea catchment is facilitated by the progressive precipitation of calcite. Notwithstanding the undersaturation of majority of the samples with respect to fluorite and calcite, the strong positive correlation (r = 0.45) between SI fluorite and SI calcite further highlights the role calcite plays in the F^- concentrations in the groundwater (Fig. 7c). Therefore, F^- and Ca^{2+} have a direct relationship. The groundwater is also undersaturated with respect to dolomite as observed in the cross plot of the SI dolomite versus F^- concentrations (Fig. 7d) suggesting the prevalence of ambient conditions necessary for calcite dissolution (Lermi and Ertan, 2019). Almost 91% of the samples are saturated with respect to albite, reflecting the dominance of silicate weathering in the aquifer (Fig. 7e). It also highlights the role granitoids in the area (Fig. 1) play in the chemistry of the groundwater. F^- enrichment in the groundwater seems to be related to albite dissolution in view of the positive correlation (r = 0.095) between SI albite and F^- concentrations and also confirms the dominance of ion exchange reactions in the hydrogeological system of the Vea catchment. Undersaturation of groundwater with respect to halite (Fig. 7f) may be due to higher halite solubility, which enhanced halite dissolution to release Na^+ and Cl^- in the groundwater.

3.7. Multivariate statistical analysis

Factor analysis with principal component analysis as the extraction method was applied to the hydrochemical parameters to show their relationships and determine the factors responsible for each association. Using the Kaiser Criterion (Kaiser, 1960), three principal components with eigenvalues >1.0 but less than 2.0 and total variance of 74.9% were extracted (supplementary Table 2). The first principal component accounts for about 13.2% of the total variance and correlates positively with all the hydrochemical parameters with very strong positive loadings on EC, TDS, Na^+, K^+, Ca^{2+}, HCO_3^-, and NO_3^- (supplementary Table 2; Fig. 8). It is well established that such association of hydrochemical parameters is as a result of weathering, ion exchange reactions and intense water-rock interaction (Yidana et al., 2010). However, the association of NO_3^- with other hydrochemical parameters in the first principal component may be pointing to input from domestic sewage and nitrate fertilizers applied on farms in the Vea catchment (Zango et al., 2019). The second principal component accounts for 12.7% of the total variance and positively correlates with TDS, Na^+, Mg^{2+}, and F^- with very strong positive loadings on Cl^- and SO_4^{2-} (supplementary Table 2; Fig. 8). This kind of association also suggests the dominance of ion exchange reactions, silicate weathering and dissolution of fluoride-rich minerals such as fluorite and biotite (Laxmankumar et al., 2019) in the area. But the strong positive correlation of SO_4^{2-} with other hydrochemical parameters in the second principal component might also be giving a hint to anthropogenic contribution to the groundwater chemistry through the application of sulphate fertilizers on farmlands since the people are mainly farmers. The third principal component, which accounts for 8.39% of the total variance loads positively on EC, TDS, SO_4^{2-}, HCO_3^-, and strongly correlates with pH, temperature, Mg^{2+}, and F^- (supplementary Table 2; Fig. 8). This suggests that reverse ion exchange reactions are prevalent in the area. However, the association of SO_4^{2-} in this group further highlights anthropogenic contribution from agricultural activities to the groundwater chemistry.

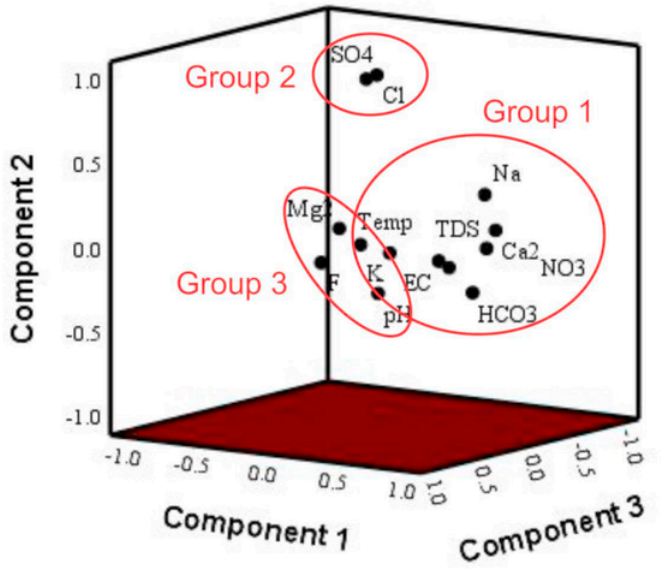

Fig. 8. Principal components extracted from R-mode factor analysis rotated in space using Varimax rotation.

3.8. Verification from isotopic compositions

The summary of $\delta^{18}O$ and δ^2H compositions of the groundwater is presented in Table 2. The $\delta^{18}O$ and δ^2H values with respect to V-SMOW vary between −4.15 and −2.75‰ and −22.5 and −13.7‰, respectively suggesting considerable isotopic variation of the groundwater. Most of the samples plot along or near the GMWL and LMWL and mostly in between the two meteoric water lines (Fig. 9a) indicating their meteoric water origin (Qian et al., 2014; Salifu et al., 2017). This implies that groundwater in the Vea catchment is likely recharged from fresh local precipitation (rainfall). However, some of the samples shifted from the GMWL and plotted in the lower slope area along the evaporation line suggesting that after precipitation, the water goes through secondary evaporation (Younas et al., 2019). Therefore, F^- in the groundwater may be released from the aquifer materials via local meteoric recharge and to some extent, evaporation. Furthermore, a plot of $\delta^{18}O$ and F^- concentrations indicates that higher groundwater F^- concentrations are fairly homogenized relative to the $\delta^{18}O$ and thus, low $\delta^{18}O$ values (Fig. 9b). The enriched isotopic composition is observed with the low fluoride concentrations whilst the depleted isotopic composition is with higher concentrations of fluoride (Table 2). Accordingly, mixing of groundwater with fast vertically recharged water and surface water along the groundwater flow conduits may be accounting for this trend (Xie et al., 2013). Such observation has already been reported by Clark and Fritz (2013) and Goller et al. (2005).

4. Conclusion and recommendations

This study was conducted to understand the source of high fluoride in groundwater within the Vea catchment of northeastern Ghana. This involved petrographic analysis of rock samples, hydrochemical analysis, multivariate statistical analysis, and stable isotope analysis. The area is mainly composed of biotite-rich granitoids of the Paleoproterozoic Birimian Supergroup. The petrographic studies show in decreasing compositional order: quartz, microcline (K-rich), plagioclase (Na-rich), biotite (Mg-rich), muscovite (Ca/Mg-rich), hornblende (Mg-rich) and other accessory minerals. The major cations vary in the order of $Na^+ > Ca^{2+} > Mg^{2+} > K^+$ whereas the major anions vary in the order $Cl^- > SO_4^{2-} > HCO_3^-$. Na–Ca–HCO3 water is dominant in the area. The fluoride concentrations vary from 0.35 to 3.95 mg/L with a mean concentration of 1.68 mg/L in excess of the maximum permissi-

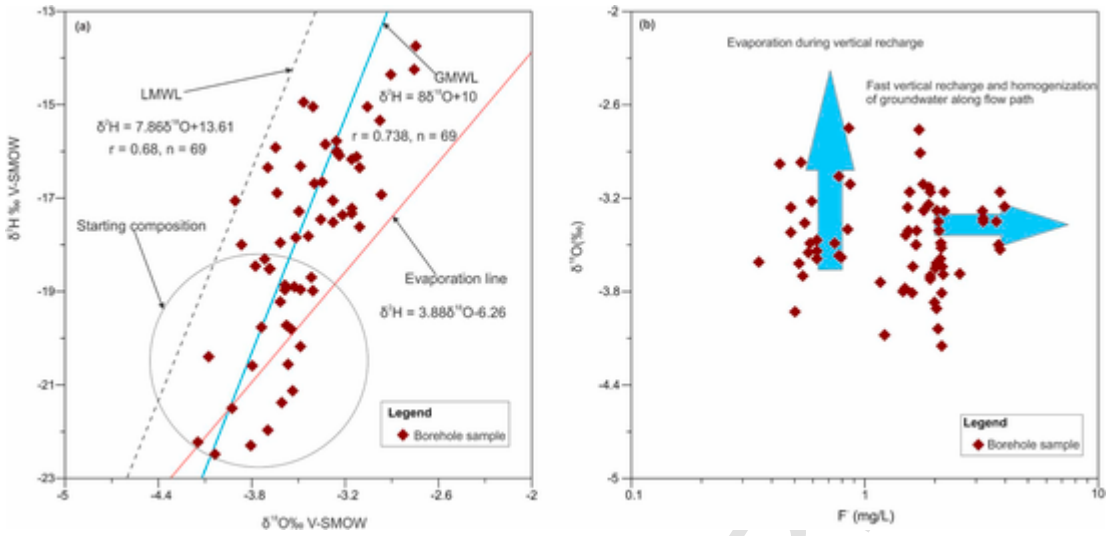

Fig. 9. Relationship between (a) δ^2H and $\delta^{18}O$ and (b) $\delta^{18}O$ and F^- (mg/L) of the groundwater samples from the Vea catchment.

ble limit of 1.5 mg/L. The fluoride contamination affected a total of 43 boreholes in the study area representing about 61% of all boreholes where the samples were collected. The affected communities are located in the northeastern, central and southwestern parts of the Vea catchment. The hydrochemical and isotopic data reveal that the groundwater evolved under high impact of water-rock interaction, ion exchange reactions, kaolinization, and silicate weathering. Moreover, evaporation after precipitation is another major process causing the enrichment of the ions in the water. All these geogenic processes resulted in the mobilization of fluoride in the groundwater in elevated levels. Saturation indices of the mineral phases in the water indicated that the groundwater is supersaturated with respect to albite due to silicate weathering and undersaturated with respect fluorite and calcite. This enhanced ion exchange and fluoride enrichment from progressive calcite precipitation. The high groundwater fluoride in the Vea catchment exposes the people to dental fluorosis, which jeopardizes the health and livelihood of the people. Therefore, the stakeholders and decision-makers in the area must come to the aid of the people by devising technologically cost-effective methods of minimizing the groundwater fluoride such as rainwater harvesting facilities, supply of drinking water from low fluoride surface water sources, and use of solar energy powered electrolytic de-fluoridation technology in the high fluoride communities.

Declaration of competing interest

The authors declare that they have no known competing financial interests or personal relationships that could have appeared to influence the work reported in this paper.

Acknowledgment

Musah Saeed Zango and Maxwell Anim-Gyampo acknowledge the support of the Earth Science department of the Faculty of Earth and Environmental Sciences, CK Tedam University of Technology and Applied Sciences, Ghana for logistics support during the field mapping and water sample collection. The Editors and anonymous Reviewers are acknowledged for their valuable comments that improved the quality of the paper.

Appendix A. Supplementary data

Supplementary data to this article can be found online at https://doi.org/10.1016/j.gsd.2020.100526.

Uncited references

, ,

References

Adimalla, N., Li, P., 2019. Occurrence, health risks, and geochemical mechanisms of fluoride and nitrate in groundwater of the rock-dominant semi-arid region, Telangana State, India. Hum. Ecol. Risk Assess. 25 (1–2), 81–103.

Akiti, T.T., 1986. Environmental isotope study of ground water in crystalline rocks of the Accra plains, Ghana. In: Proceedings of the 4th Working Meeting, Isotopes in Nature (Leipzig).

Apambire, W.B., Boyle, D.R., Michel, F.A., 1997. Geochemistry, genesis, and health implications of fluoriferous groundwaters in the upper regions of Ghana. Environ. Geol. 33, 13–24.

Chae, G.T., Yun, S.T., Kwon, M.J., Kim, Y.S., Mayer, B., 2006. Batch dissolution of granite and biotite in water: implication for fluorine geochemistry in groundwater. Geochem. J. 40 (1), 95–102.

Chae, G.T., Yun, S.T., Mayer, B., Kim, K.H., Kim, S.Y., Kwon, J.S., Koh, Y.K., 2007. Fluorine geochemistry in bedrock groundwater of South Korea. Sci. Total Environ. 385 (1–3), 272–283.

Clark, I.D., Fritz, P., 2013. Environmental Isotopes in Hydrogeology. CRC press.

Craig, H., 1961. Isotopic variations in meteoric waters. Science 133 (3465), 1702–1703.

Craig, L., Thomas, J.M., Lutz, A., Decker, D.L., 2018. Determining the optimum locations for pumping low-fluoride groundwater to distribute to communities in a fluoridic area in the Upper East Region, Ghana. Chem. Geol. 476, 481–492.

Dehbandi, R., Moore, F., Keshavarzi, B., 2018. Geochemical sources, hydrogeochemical behavior, and health risk assessment of fluoride in an endemic fluorosis area, central Iran. Chemosphere 193, 763–776.

Dickson, K., Benneh, G., 1995. A New Geography of Ghana. Longman, UK, pp. 21–33.

Enalou, H.B., Moore, F., Keshavarzi, B., Zarei, M., 2018. Source apportionment and health risk assessment of fluoride in water resources, south of Fars province, Iran: stable isotopes (δ18O and δD) and geochemical modeling approaches. Appl. Geochem. 98, 197–205.

Farooqi, A., Masuda, H., Firdous, N., 2007. Toxic fluoride and arsenic contaminated groundwater in the Lahore and Kasur districts, Punjab, Pakistan and possible contaminant sources. Environ. Pollut. 145 (3), 839–849.

Freeze, R.A., Cherry, J.A., 1979. Groundwater. Prentice Hall, Englewood Cliffs, NJ 07632.

Ganyaglo, S.Y., Gibrilla, A., Teye, E.M., Owusu-Ansah, E.D.G.J., Tettey, S., Diabene, P.Y., Asimah, S., 2019. Groundwater fluoride contamination and probabilistic health risk assessment in fluoride endemic areas of the Upper East Region, Ghana. Chemosphere 233, 862–872. doi:10.1016/j.chemosphere.2019.05.276.

Gibbs, R.J., 1970. Mechanisms controlling world water chemistry. Science 170, 1088–1090.

Goller, R., Wilcke, W., Leng, M.J., Tobschall, H.J., Wagner, K., Valarezo, C., Zech, W., 2005. Tracing water paths through small catchments under a tropical montane rain forest in south Ecuador by an oxygen isotope approach. J. Hydrol. 308 (1–4), 67–80.

Hounslow, A., 1995. Water Quality Data: Analysis and Interpretation. CRC Press LLC, Lewis Publishers, p. 397.
IAEA, 2009. Laser spectroscopic analysis of liquid water samples for stable hydrogen and oxygen isotopes. Isotope Hydrology Section. International Atomic Energy Agency 49.
Kaiser, H.F., 1960. The application of electronic computers to factor analysis. Educ. Psychol. Meas. 20 (1), 141–151.
Karro, E., Uppin, M., 2013. The occurrence and hydrochemistry of fluoride and boron in carbonate aquifer system, central and western Estonia. Environ. Monit. Assess. 185 (5), 3735–3748.
Keshavarzi, B., Moore, F., Esmaeili, A., Rastmanesh, F., 2010. The source of fluoride toxicity in Muteh area, Isfahan, Iran. Environmental Earth Sciences 61 (4), 777–786.
Kesse, G.O., 1985. The Mineral and Rock Resources of Ghana. A.A. Balkema, Rotterdam.
Koffi, K.V., Obuobie, E., Banning, A., Wohnlich, S., 2017. Hydrochemical characteristics of groundwater and surface water for domestic and irrigation purposes in Vea catchment, Northern Ghana. Environmental Earth Sciences 76 (4), 185.
Koritnig, S., 1978. Fluorine. Pages 9-C-1 to B-9-O-3. In: Wedepohl, K.H. (Ed.), Handbook of Geochemistry, II/1. Springler-Verlag, Berlin.
Krauskopf, K.B., Bird, D.K., 1995. An Introduction to Geochemistry. McGraw-Hill Int., Singapore, p. 647.
Kumar, S., Singh, R., Venkatesh, A.S., Udayabhanu, G., Sahoo, P.R., 2019. Medical Geological assessment of fluoride contaminated groundwater in parts of Indo-Gangetic Alluvial plains. Sci. Rep. 9 (1), 1–16.
Kumar, S., Venkatesh, A.S., Singh, R., Udayabhanu, G., Saha, D., 2018. Geochemical signatures and isotopic systematics constraining dynamics of fluoride contamination in groundwater across Jamui district, Indo-Gangetic alluvial plains, India. Chemosphere 205, 493–505.
Kundu, M.C., Mandal, B., 2009. Agricultural activities influence nitrate and fluoride contamination in drinking groundwater of an intensively cultivated district in India. Water Air Soil Pollut. 198 (1–4), 243–252.
Laxmankumar, D., Satyanarayana, E., Dhakate, R., Saxena, P.R., 2019. Hydrogeochemical characteristics with respect to fluoride contamination in groundwater of Maheshwarm mandal, RR district, Telangana state, India. Groundwater for Sustainable Development 8, 474–483.
Lermi, A., Ertan, G., 2019. Hydrochemical and isotopic studies to understand quality problems in groundwater of the Niğde Province, Central Turkey. Environmental Earth Sciences 78 (12), 365.
Leube, A., Hirdes, W., Mauer, R., Kesse, G.O., 1990. The early Proterozoic Birimian Supergroup of Ghana and some aspects of its associated gold mineralization. Precambrian Res. 46, 139–165.
Li, P., He, X., Li, Y., Xiang, G., 2019. Occurrence and health implication of fluoride in groundwater of loess aquifer in the Chinese loess plateau: a case study of Tongchuan, Northwest China. Exposure and Health 11 (2), 95–107.
Li, Y.H., Wang, S., Zhang, X., Wei, J., Xu, C., Luan, Z., Wu, D., 2003. Adsorption of fluoride from water by aligned carbon nanotubes. Mater. Res. Bull. 38 (3), 469–476.
Martin, N., Van De Giesen, N., 2005. Spatial distribution of groundwater production and development potential in the Volta River basin of Ghana and Burkina Faso. Water Int. 30 (2), 239–249.
Martins, V.T.D.S., Pino, D.S., Bertolo, R., Hirata, R., Babinski, M., Pacheco, D.F., Rios, A.P., 2018. Who to blame for groundwater fluoride anomaly in São Paulo, Brazil? Hydrogeochemistry and isotopic evidence. Appl. Geochem. 90, 25–38.
Milési, J.P., Feybesse, J.L., Ledru, P., Dommanget, A., Oue-draogo, M.F., Marcoux, E., Prost, A., Vinchon, C., Syl-vain, J.P., Johan, V., Tegyey, M., Calvez, J.P., Lagny, P.H., 1989. West African gold deposits in their Lower Proterozoic lithostructural setting. Chron. Rech. Min. 497, 3–98.
Naseem, S., Rafique, T., Bashir, E., Bhanger, M.I., Laghari, A., Usmani, T.H., 2010. Lithological influences on occurrence of high-fluoride groundwater in Nagar Parkar area, Thar Desert, Pakistan. Chemosphere 78, 1313–1321.
Olaka, L.A., Wilke, F.D., Olago, D.O., Odada, E.O., Mulch, A., Musolff, A., 2016. Groundwater fluoride enrichment in an active rift setting: Central Kenya Rift case study. Sci. Total Environ. 545, 641–653.
Ozsvath, D.L., 2006. Fluoride concentration in a crystalline bedrock aquifer Marathon Country, Wisconsin. Environ. Geol. 50, 132–138.
Parkhurst, D.L., Appelo, C.A.J., 1999. User's guide to PHREEQC (Version 2): a computer program for speciation, batch-reaction, one-dimensional transport, and inverse geochemical calculations. Water-resources investigations report 99 (4259), 312.
Piper, A.M., 1953. A Graphic Procedure in the Geochemical Interpretation of Water Analysis. US Geological Survey, Washington DC.
Qian, H., Wu, J., Zhou, Y., Li, P., 2014. Stable oxygen and hydrogen isotopes as indicators of lake water recharge and evaporation in the lakes of the Yinchuan Plain. Hydrol. Process. 28 (10), 3554–3562.
Raju, N.J., Dey, S., Das, K., 2009. Fluoride contamination in groundwaters of sonbhadra district, Uttar Pradesh, India. Curr. Sci. 96 (7), 979–985.
Rao, N.S., Marghade, D., Dinakar, A., Chandana, I., Sunitha, B., Ravindra, B., Balaji, T., 2017. Geochemical characteristics and controlling factors of chemical composition of groundwater in a part of Guntur district, Andhra Pradesh, India. Environmental Earth Sciences 76 (21), 747.
Salifu, M., Yidana, S.M., Anim-Gyampo, M., Appenteng, M., Saka, D., Aidoo, F., Sarfo, M., 2017. Hydrogeochemical and isotopic studies of groundwater in the middle voltaian aquifers of the Gushegu district of the Northern region. Applied Water Science 7 (3), 1117–1129.
Saxena, U., Saxena, S., 2014. Ground water quality evaluation with special reference to Fluoride and Nitrate contamination in Bassi Tehsil of district Jaipur, Rajasthan, India. Int. J. Environ. Sci. 5 (1), 67.
Shah, M.T., Danishwar, S., 2003. Potential fluoride contamination in the drinking water of Naranji area, northwest frontier province, Pakistan. Environ. Geochem. Health 25 (4), 475–481.
Su, H., Wang, J., Liu, J., 2019. Geochemical factors controlling the occurrence of high-fluoride groundwater in the western region of the Ordos basin, northwestern China. Environ. Pollut. 252 (Part B), 1154–1162. doi:10.1016/j.envpol.2019.06.046.
Sunkari, E.D., Abu, M., 2019. Hydrochemistry with special reference to fluoride contamination in groundwater of the Bongo district, Upper East Region, Ghana. Sustainable Water Resources Management 5 (4), 1803–1814. doi:10.1007/s40899-019- 00335-0.
Sunkari, E.D., Abu, M., Bayowobie, P.S., Dokuz, U.E., 2019. Hydrogeochemical appraisal of groundwater quality in the Ga west municipality, Ghana: implication for domestic and irrigation purposes. Groundwater for Sustainable Development 8, 501–511.
Sunkari, E.D., Abu, M., Zango, M.S., Wani, A.M.L., 2020. Hydrogeochemical characterization and assessment of groundwater quality in the kwahu-bombouaka group of the voltaian Supergroup, Ghana. J. Afr. Earth Sci. 103899. doi:10.1016/j.jafrearsci.2020.103899.
Sunkari, E.D., Zango, M.S., Korboe, H.M., 2018. Comparative analysis of fluoride concentrations in groundwaters in Northern and Southern Ghana: implications for the contaminant sources. Earth Systems and Environment 2 (1), 103–117.
Thivya, C., Chidambaram, S., Rao, M.S., Thilagavathi, R., Prasanna, M.V., Manikandan, S., 2017. Assessment of fluoride contaminations in groundwater of hard rock aquifers in Madurai district, Tamil Nadu (India). Applied Water Science 7 (2), 1011–1023.
World Health Organization-Who, 2017. Guidelines for Drinking-Water Quality: Fourth Edition Incorporating the First Addendum. WHO, Geneva.
Xie, X., Wang, Y., Su, C., Duan, M., 2013. Effects of recharge and discharge on δ2H and δ18O composition and chloride concentration of high arsenic/fluoride groundwater from the Datong Basin, Northern China. Water Environ. Res. 85 (2), 113–123.
Yidana, S.M., Banoeng-Yakubo, B., Akabzaa, T.M., 2010. Analysis of groundwater quality using multivariate and spatial analyses in the Keta basin, Ghana. J. Afr. Earth Sci. 58 (2), 220–234.
Younas, A., Mushtaq, N., Khattak, J.A., Javed, T., Rehman, H.U., Farooqi, A., 2019. High levels of fluoride contamination in groundwater of the semi-arid alluvial aquifers, Pakistan: evaluating the recharge sources and geochemical identification via stable isotopes and other major elemental data. Environ. Sci. Pollut. Control Ser. 1 14. doi:10.1007/s11356-019-06610-z.
Young, S.M., Pitawala, A., Ishiga, H., 2011. Factors controlling fluoride contents of groundwater in north-central and northwestern Sri Lanka. Environmental Earth Sciences 63 (6), 1333–1342.
Zango, M.S., Sunkari, E.D., Abu, M., Lermi, A., 2019. Hydrogeochemical controls and human health risk assessment of groundwater fluoride and boron in the semi-arid North East region of Ghana. J. Geochem. Explor. 207, 106363.